Published in final edited form as:
Biochemistry. 2013 September 17; 52(37): . doi:10.1021/bi400444y.

Site-Directed Mutagenesis of Catalytic Residues in N^5-Carboxyaminoimidazole Ribonucleotide Synthetase

Mahender B. Dewal[‡] and **Steven M. Firestine**[*]
[1]Department of Pharmaceutical Sciences, Eugene Applebaum College of Pharmacy and Health Sciences, Wayne State University, Detroit, MI 48201

Abstract

N^5-CAIR synthetase, an essential enzyme in microorganisms, converts 5-aminoimidazole ribonucleotide (AIR) and bicarbonate to N^5-CAIR with the aid of ATP. Previous X-ray crystallographic analyses of *Aspergillus clavatus* N^5-CAIR synthetase postulated that R271, H273, and K353 were important for bicarbonate binding and for catalysis. As reported here, site-directed mutagenesis of these residues revealed that R271 and H273 are, indeed, critical for bicarbonate binding and catalysis whereas all K353 mutations, even ones conservative in nature, are inactive. Studies on the R271K mutant protein revealed cooperative substrate inhibition for ATP with a K_i of 1.2 mM. Kinetic investigation of the H273A mutant protein indicated that it was cooperative with respect to AIR; however, this effect was not seen in either the wild-type or any of the other mutant proteins. Cooperative ATP-dependent inhibition of wild-type N^5-CAIR synthetase was also detected with ATP displaying a K_i of 3.3 mM. Taken together, these results indicate that N^5-CAIR synthetase operates maximally within a narrow concentration of ATP.

Keywords

synthetase; carboxylase; mutagenesis; carboxyaminoimidazole; cooperativity; substrate inhibition

Introduction

N^5-carboxyaminoimidazole ribonucleotide (N^5-CAIR) synthetase catalyzes the sixth step in microbial *de novo* purine biosynthesis, namely the ATP-dependent carboxylation of 5-aminomidazole ribonucleotide (AIR) to produce the chemically unstable intermediate, N^5-CAIR (Scheme 1). N^5-CAIR synthetase belongs to the ATP-grasp superfamily of enzymes which includes two other carboxylase enzymes, biotin carboxylase and carbamoyl phosphate synthetase (1-3). Crystallographic investigations on N^5-CAIR synthetase from both bacteria and fungi indicate that the enzyme displays close structural similarity to these two enzymes and like biotin carboxylase, the enzyme exists as a dimer. Interestingly, N^5-CAIR synthetase is also structurally related to other enzymes in the *de novo* purine pathway suggesting that these enzymes may have evolved from a common ancestral protein (4, 5).

To whom correspondence should be addressed: Steven M. Firestine, Department of Pharmaceutical Sciences, Eugene Applebaum College of Pharmacy and Health Sciences, Wayne State University, 259 Mack Avenue, Detroit, MI 48201, USA, Tel.: (313) 577-0455; Fax.: (313) 577-2033; sfirestine@wayne.edu.
[‡]Author's present address: Department of Chemistry, Massachusetts Institute of Technology, Cambridge, MA 02139
[*]This research was supported in part by NIH grant (GM087467 to S. M. F.)

Supporting Information. Primers used for the construction of the mutants and the protease digestion of both wild-type and mutated proteins. Protease digestion of mutated proteins in the presence of various substrates is also included. This material is available free of charge via the Internet at http://pubs.acs.org.

Past structural investigations on the N^5-CAIR synthetases from *Escherichia coli* and *Aspergillus clavatus* provided detailed information on the architecture of the active site (Figure 1) (6, 7). These studies highlighted three conserved residues, R271, H273, and K353 (*A. clavatus* numbering), which were oriented in the active site region between the AIR and ATP binding sites and thus likely to be involved in bicarbonate binding and catalysis. Modeling using the information from *E. coli* N^5-CAIR synthetases complexed with ADP:P_i (3ETJ) validated this hypothesis and provided a hypothetical location for the intermediate, carboxyphosphate (Figure 1). Based upon this model, we proposed a mechanism for N^5-CAIR synthetase in which bicarbonate is first bound by R271 followed by attack onto the γ-phosphate of ATP to generate carboxyphosphate (Figure 2) (7). H273, which is located near the γ-phosphate of ATP, could aid in the binding of bicarbonate by electrostatic interactions and/or could facilitate catalysis by interacting with E256, a conserved magnesium-binding residue. Once carboxyphosphate is formed, we hypothesized that it decomposes to carbon dioxide, which is stabilized by K353 and R271. Carbon dioxide is then attacked by AIR with the aid of D153. Whereas the structural studies provided solid evidence for the proposed mechanism, the only site-directed mutagenesis experiments that were conducted on N^5-CAIR synthetase focused on identifying the roles of amino acids in the AIR-binding site (7). Site-directed mutagenesis studies of H273 and R271 were not conducted, and only a single mutation at K353 (K353A) was investigated (7). Thus, in the current report, we examine the function of R271, H273, and K353 in the mechanism of N^5-CAIR synthetase. Our results indicate that these residues play a key role in bicarbonate binding and in the overall reaction of the enzyme. Furthermore, several mutant proteins displayed unique kinetics which suggests that there may be cooperativity between the two subunits of the N^5-CAIR synthetase dimer as well as an optimal concentration of ATP under which the enzyme is maximally active.

Experimental Procedures

Materials

Ampicillin sodium salt, B-PER (Pierce Biotechnologies) and Amicon Ultra centrifugal filters were purchased from Fisher Scientific. Isopropyl β-D-1-thiogalactopyranoside (IPTG) and HisPur Cobalt resin were purchased from Gold Biotechnology (USA). ATP (99.9%), PEP, and streptomycin sulfate were purchased from Sigma-Aldrich. NADH was purchased from Acros. AIR was prepared as previously described and was estimated to be 95% pure based upon HPLC analysis (8). Total CO_2/bicarbonate levels in the assays were determined using the L3K CO_2 quantitation kit (Sekisui Diagnostics) following the manufacturers protocol.

Construction of N^5-CAIR Synthetase Mutant Proteins

The *Aspergillus* N^5-CAIR synthetase-pET28 plasmid with an N-terminal His tag of the following sequence (MGSSHHHHHHSSENLYFQGH) was used to generate the required mutant proteins. These mutant proteins were generated by the Quikchange II site-directed mutagenesis protocol (Stratagene, La Jolla, CA) using primers (Supplemental information) designed to incorporate the selected mutation. The nucleotide sequence of each mutant protein was verified by DNA sequencing to confirm that the desired mutation was made and no other mutation was incorporated during the polymerase chain reaction (PCR).

Protein Expression and Purification

E. coli BL21(DE3) pLysS cells were transformed with the N^5-CAIR synthetase-pET28 plasmids (wild-type or mutant) and plated onto Luria Broth (LB) agar containing 100 μg/mL of ampicillin. An individual colony was selected and grown overnight in LB media containing 100 μg/mL of ampicillin. The overnight cultures were used to inoculate (1%) a 2

L culture supplemented with 100 μg/mL of ampicillin, which was grown, with shaking at 37 °C, until an optical density of 0.2 was obtained. The cultures were then cooled to 25 °C and expression was induced with the addition of IPTG to a final concentration of 1.0 mM. The induction was allowed to proceed for 5 hr at 25 °C. The cells were harvested by centrifugation at 2,700 g at 4 °C for 15 min, and the cell pellet was stored at -20 °C.

For purification, the cell pellets were resuspended in B-PER (10 mL/250 mL of cell culture, Pierce Biotechnology) to extract the cell content, and the cell debris was removed by centrifugation at 27,000 g for 45 min. A solution of streptomycin sulfate was subsequently added to the supernatant to a final concentration of 1% (w/v) and the mixture was incubated at 4 °C (with occasional shaking at 10 min intervals) for 30 min. The precipitated material was removed by centrifugation at 27,000 g for 45 min. The supernatant was loaded on to a pre-washed (3 column volumes with wash buffer, 50 mM sodium phosphate, 300 mM NaCl, 10 mM imidazole, pH 7.4) 2.0 cm × 4.0 cm HisPur Cobalt resin column. The column was washed with 3 column volumes of buffer (50 mM sodium phosphate, 300 mM NaCl, 25 mM imidazole, pH 7.4), and the protein was eluted by addition of elution buffer (50 mM sodium phosphate, 300 mM NaCl, 100 mM imidazole, pH 7.4). Fractions containing significant amounts of the desired protein, as determined by SDS-PAGE, were pooled and dialyzed overnight against 3 L of buffer (10 mM Tris HCl, 200 mM NaCl, pH 8.0). The dialyzed protein was concentrated using Amicon Ultra centrifugal filters (10,000 MWCO), and the concentration of the protein determined by Bradford assay (9). The protein was judged to be approximately 98% pure based upon an overloaded SDS-PAGE gel.

Enzyme Assays

The full and partial reactions catalyzed by N^5-CAIR synthetase were monitored by the well-known coupled assay systems, which measure the rate of ATP consumption as a function of ADP production and AIR consumption (**Scheme I**) (10-12). For the AIR-dependent full reaction, initial rates of N^5-CAIR formation were determined at various concentrations of AIR (2.5 μM to 3.0 mM depending on the mutant protein) in buffer (50 mM Hepes, pH 7.8) containing 1 mM ATP, 2 mM PEP, 0.2 mM NADH, 5 units of pyruvate kinase, 7 units of lactate dehydrogenase and 1 mM $NaHCO_3$ at 37 °C. For the ATP-dependent full reaction, initial rates were determined using the same conditions except that the concentration of ATP was varied (5.0 μM to 5.0 mM depending on the mutant protein) while the concentration of AIR was kept constant (saturated level of that particular mutant protein). For the bicarbonate-stimulated ATPase activity, the initial rates were determined by varying the concentration of $NaHCO_3$ (0.1 mM to 100 mM) while ATP was held at a fixed concentration (1mM). The background concentration of bicarbonate was determined using the L3K CO_2 kit which measures the amount of bicarbonate in solution using the coupled PEP carboxylase/malate dehydrogenase assay system. The background level of bicarbonate was found to be 0.21 mM. This value was added to each amount of bicarbonate added in the assay to determine the total amount of bicarbonate in solution.

Data Analysis

The kinetic parameters, V_{max} and K_m, were determined by the least-square nonlinear regression method. The best-fit lines were plotted for the initial rate versus substrate concentration data using Kaleidagraph. For the mutant proteins that displayed hyperbolic curves, the data were fitted to the Michaelis-Menten equation (eqn 1). K_{cat} values were calculated using a dimer molecular weight of 90 KDa. For the H273A mutant protein, the data were fitted to equation 2. The R271K mutant protein displays substrate inhibition. Equations 3 and 4, which describe substrate inhibition and partial substrate inhibition respectively, failed to give an acceptable fit to the data for the R271K mutant. Ultimately, the data were fitted to equation 5 for cooperative substrate inhibition. In all of the equations,

V_{max} is the maximum velocity, K_m is the Michaelis constant, [S] is the substrate concentration, v_0 is the initial velocity, K_i is the inhibition constant and n is the Hill coefficient.

$$v_0 = \frac{V_{max}[S]}{K_m + [S]} \quad \text{eq. 1}$$

$$v_0 = \frac{V_{max}[S]^n}{K_m + [S]^n} \quad \text{eq 2}$$

$$v_0 = \frac{V_{max}[S]}{K_m + [S] + \frac{[S]^2}{K_i}} \quad \text{eq 3}$$

$$v_0 = \frac{V_{max} + V_{min}\left(\frac{[S]}{K_i}\right)}{1 + \frac{K_m}{[S]} + \frac{[S]}{K_i}} \quad \text{eq 4}$$

$$v_0 = \frac{V_{max}}{1 + \frac{K_m}{[S]} + \frac{[S]^n}{K_i^n}} \quad \text{eq 5}$$

Proteolysis Assay

To a microcentrifuge tube, 14 μg of either wild-type or mutated protein were added to a buffer (50 mM Hepes, pH 7.8, 20 mM KCl, and 0.6 mM $MgCl_2$) such that the total volume was 30 μL. To this, 0.14 μg of protease (subtilisin from *Bacillus licheniformis*, Sigma) was added, and the reactions were incubated on ice for 60 min. The proteolysis reaction was quenched with 1 mM PMSF, and the products were separated using a denaturing 12% SDS-PAGE gel. The protease data is shown in Supplemental Information.

Results

Identification of Residues for Site-Directed Mutagenesis

Recently, the crystal structures of *A. clavatus* N^5-CAIR synthetase complexed with either MgATP (PDB code 3K5H) or MgADP and the substrate AIR (PDB code 3K5I) was reported (7). Based on the structural information from these crystal structures, we performed site-directed mutagenesis on selected residues found in the AIR binding site (E73, Y152, D153, R155 and K353) (7). These studies identified D153 as the active site base and highlighted the role of Y152 in binding of the substrate. The role of K353 could not be ascertained because the mutant was inactive, but still bound AIR, which indicated that the enzyme folded properly. This suggested that K353 was involved in catalysis and likely played a role in either bicarbonate binding or the reaction of bicarbonate with ATP. The structural studies also indicated that the conserved residues R271 and H273 were located in the active site between the ATP and AIR binding sites (Figure 1). To examine the roles of these residues in catalysis, R271, H273, and K353 were mutated (see Table 1-3 for mutants created) and subjected to kinetic analysis to determine the function of the residues in substrate binding and catalysis.

Half Reaction Catalyzed by N^5-CAIR Synthetase

ATP hydrolysis is a required step for the carboxylation of AIR to produce N^5-CAIR (**Scheme I**). Conceptually, the first step is the reaction of bicarbonate with ATP to generate the intermediate, carboxyphosphate. This half-reaction can be measured based upon the consumption of ATP in the absence of the substrate, AIR. The ATPase activity observed for N^5-CAIR synthetase is also seen in two other ATP-grasp carboxylase enzymes, biotin carboxylase and carbamoyl phosphate synthetase (13-18). The kinetics of the half-reaction for both wild-type and mutated N^5-CAIR synthetases are reported in Table 1. To determine whether the mutated proteins were folded, we subjected each one to proteolysis by the non-specific protease, subtilisin, for 60 minutes (Supplemental Information). Under these conditions, approximately 60% of wild-type N^5-CAIR synthetase was digested into two main protein fragments. Digestion of mutant proteins Y152F, R271Q, R271K and H273Q gave cleavage patterns which were qualitatively identical to that for the wild-type enzyme. Treatment of R271A, K353R and H273A mutant proteins with the protease resulted in a substantial change in the relative abundance of the digested fragments but not an alteration in the size of the fragments. Taken together, the protease assay indicates that these mutants are folded properly but, in some instances, may have altered flexibility compared to the wild-type protein.

The bicarbonate-stimulated ATPase activity of wild-type N^5-CAIR synthetase was 1,300-fold slower than the ATPase activity for the full reaction indicating that AIR binding enhances the ATPase activity of the enzyme. We were unable to detect ATPase activity for mutant proteins R271A, R271Q, H273A, H273Q, K353R, and K353A. Based upon our experimental conditions and our detection limit, this indicates that the rate of catalysis of these proteins is less than 0.00013 μmol min^{-1} mg^{-1}. However, the R271K protein did display detectable activity although the k_{cat}/K_m was 1,000-fold lower than the wild-type enzyme. The K_m for bicarbonate also increased suggesting that R271 plays a role in bicarbonate binding.

From the crystal structure, it has been shown that E73, Y152, and R155 form hydrogen bonds to AIR, a result supported by kinetic studies on E73A, Y152A, and R155A mutant proteins (7). Here we have investigated the effect of these mutations on the bicarbonate dependent half reaction (Table 1). The catalytic efficiency for these mutants are comparable to the wild-type enzyme although the E73A and D153A mutants displayed an enhanced ATPase rate but at the expense of bicarbonate binding.

Full Reaction Catalyzed by N^5-CAIR Synthetase

We investigated the kinetics of the mutant proteins for the full reaction of N^5-CAIR synthetase. The results are shown in Tables 2 and 3. For the AIR-dependent reaction, Y152F displayed a 10-fold lower catalytic efficiency and a 3-fold change in K_m. These values are modest compared to the Y152A protein, which displayed 660-fold change in efficiency with a change of 18-fold in the K_m for AIR. These data highlight the value of the aromatic stacking interaction for AIR binding to the enzyme. The K353A and K353R mutant proteins were inactive. Unlike the half-reaction, activity of the R271A, R271Q, R271K and H273Q mutants could be measured although the catalytic efficiencies were 3,000 to 460,000-fold lower than the wild-type enzyme[1]. This indicates that these residues play crucial roles in catalysis. The H273A mutation resulted in a 34-fold change in the K_m for AIR, but for the

[1]The full reaction requires the reaction of bicarbonate with ATP to form carboxyphosphate. As shown in Table 1, we could not detect the ATPase activity in the absence of AIR for these mutants. Given the fact that AIR increases the rate of ATPase activity by approximately 1,300-fold, we can estimate the rate of ATPase activity for the half-reaction from the data in Tables 2 and 3. For the R271 mutants, the estimated rate is 100-fold below our detection limit. For the H273 mutants, the estimated rate is approximately at our detection limit and is 3-fold below the lowest measured rate displayed in any of the tables.

H273Q mutant protein, the K_m was essentially identical to observed for the wild-type enzyme. However, even though H273Q appears to be identical to the wild-type enzyme in terms of AIR binding, there is a 25,000-fold decrease in V_{max} indicating that the imidazole ring of histidine plays a critical role in catalysis. These observations suggest that the hydrogen bonding ability of H273 plays a critical role in catalysis. Interestingly, in biotin carboxylase, glutamine occurs in the same position as H273, and thus it was expected that H273Q should be functionally equivalent in N^5-CAIR synthetase.

Examination of the Michaelis-Menten kinetics of the H273A protein revealed a sigmodial curve (Figure 3) which is indicative of positive cooperative behavior. The curve of AIR concentration versus initial velocity was fitted to equation 2 with a coefficient of 2. Since N^5-CAIR synthetase exists as a dimer, we conclude that there is likely subunit-subunit cooperative behavior with one molecule of substrate bound to each dimer. Biotin carboxylase has also demonstrated cooperative behavior; however, unlike H273A, this enzyme demonstrated negative cooperative behavior with regard to bicarbonate binding (19-21). Cooperative behavior was neither observed for the wild-type enzyme nor for the H273Q mutant protein, both of which have the same K_m value for AIR. The observation of cooperativity in the H273A mutant protein could be the result of the significantly weaker binding of AIR which uncovered the cooperativity of the system or could have been induced by the mutation. However, given the fact that the H273Q mutant has the same AIR K_m as the wild-type enzyme and did not display cooperativity, we believe that the observed cooperativity is due to the weaker binding of AIR and is intrinsic to the system.

Examination of the full reaction with varied ATP concentrations revealed that for the mutant proteins R271A, R271Q, H273A, R271K and H273Q, the K_m for ATP was essentially unaltered. The mutant proteins displayed a 900 – 240,000 fold lower catalytic proficiency than the wild-type enzyme indicating that these residues play a role in bicarbonate binding and the reaction of bicarbonate with ATP.

The R271K mutant protein displayed an unique Michaelis-Menten curve indicative of substrate inhibition by ATP. Fitting the data to the equation for substrate inhibition (eq. 3) gave a poor fit (R^2=0.984, $Chi^2=6.56 \times 10^{-5}$, Figure 4A, dashed line). Fitting to the equation for partial substrate inhibition (eq. 4)(22) gave a good fit; however, V_{min} was essentially zero indicating that at infinite substrate levels, the enzyme would be completely inhibited. Finally, we discovered that fitting the data to cooperative substrate inhibition (eq. 5) gave an excellent fit (R^2=0.997, $Chi^2=1.16 \times 10^{-5}$, Figure 4A, solid line). The fit to equation 5 was best with n=2 and this fit indicated a K_i of 1.2 mM for ATP. In this equation, ATP inhibition was cooperative indicating that two molecules of ATP were needed to inhibit the system. The most likely site for a second molecule of ATP to bind is the AIR binding site. Such binding is theoretically possible because AIR is also a nucleotide, and there are substantial contacts that could be made to the phosphate group of both nucleotides. A recent structure of biotin carboxylase has demonstrated that 2 molecules of ADP bind to the active site with one molecule of ADP binding to the biotin binding site of the enzyme (23). A structural overlay of N^5-CAIR synthetase and biotin carboxylase indicates that the AIR and biotin binding sites are superimposible further supporting the assertion that the second molecule of ATP is located in the AIR binding site.

The discovery of substrate inhibition for ATP in the R271K mutant protein motivated us to investigate the wild-type enzyme at higher ATP levels. Exploration of ATP up to 5 mM revealed substrate inhibition in the wild-type enzyme. Like that observed for the R271K protein, the standard equation for substrate inhibition yielded poor fits. We again found that equation 5 led to the best fit (Figure 4B); however, for the wild-type enzyme, n=4, while the

K_i was 3.3 mM. These results suggest that substrate inhibition is more cooperative in the wild-type enzyme than in the R271K mutant protein; however, ATP was a weaker inhibitor.

Discussion

The availability of the structures of N^5-CAIR synthetase led to a hypothesis regarding the bicarbonate binding site in this enzyme. We selected three residues which we hypothesized should play a role in bicarbonate binding and the attack of bicarbonate on ATP. These residues, R271, H273, and K353 were mutated to a variety of amino acids, and the mutant proteins were analyzed for activity in both the half and full reactions. All mutant proteins, with the exception of the R271K version, were inactive in the half-reaction. Mutations made distal to the bicarbonate site resulted in proteins that were active and only minimally different from the wild-type enzyme. For the R271K mutant protein, both V_{max} and K_m for bicarbonate were altered confirming that this residue was involved in bicarbonate binding. Most of the mutant proteins did display activity in the full reaction which indicates that the enzymes were catalytically active, albeit with significant decreases in catalytic proficiencies. Together with the structural data, our mutagenesis data support the conclusion that these three residues are involved in bicarbonate binding and in aiding the attack of bicarbonate onto ATP.

The Role of R271 in Binding and Catalysis

R271 is an interesting residue. Structural studies revealed that the residue is in the bicarbonate binding pocket and likely forms a direct interaction with bicarbonate. R271 is conserved in all ATP-grasp carboxylases and the corresponding residue in biotin carboxylase is R292 (24). In biotin carboxylase, R292 forms a hydrogen bond with bicarbonate and likely helps to neutralize the charge on bicarbonate. Interestingly, when R292 was mutated to alanine in biotin carboxylase, only a modest change in the V_{max} of the half-reaction was observed, and the K_m for bicarbonate was not appreciably altered (19). In contrast, mutation of this arginine residue in carbamoyl phosphate synthetase resulted in a drastically elevated K_m for bicarbonate and a 300-fold decrease in V_{max}(25). Our results are more like those obtained for carbamoyl phosphate synthetase.

The R271K mutant protein also displayed cooperative substrate inhibition with regard to ATP binding, and the kinetics suggested that two molecules of ATP were bound for inhibition. We believe that ATP binds to the AIR-binding site of the enzyme due to the fact that both are nucleotides and a recent crystal structure of biotin carboxylase has shown that two molecules of ADP can bind to the active site; one molecule in the ATP site and the second in the biotin/bicarbonate site (23). Other enzymes which display this type of substrate inhibition include aspartate transcarbamoylase, CTP synthase, and the ATPase activity of GroEL (22, 26-28).

The Role of H273

H273 is located near the γ-phosphate of ATP and would likely be involved in the activation of ATP for the attack by bicarbonate. However, mutation of it to an alanine had modest effects on the K_m for ATP but did change the K_m for AIR even though the residue is 9 Å away from the AIR binding site. H273Q, which replaces the hydrogen bonding components removed in H273A, restored K_m for AIR but still displayed lower V_{max} values indicating that H273 is involved in catalysis. H273A displayed cooperative behavior with respect to AIR. Since N^5-CAIR synthetase is a dimer, we believe that this change resulted in either the uncovering of subunit communication between the two monomers or introduced cooperative behavior to the enzyme.

How the H273A mutation resulted in, or uncovered, cooperative behavior is unknown. However, we can speculate based upon the structure (Figure 5A). H273A is at the beginning of a helix which extends from H273 to E281. This helix, which contains a number of conserved residues, extends to the dimer boundary and is located at the bottom of the channel between the A and C domains of the protein. This helix likely serves to help close the opening between the A and C domains since several amino acids in this helix interact with both domains. In addition, several critical amino acids in both the A and C domains around the helix interact with AIR, thus providing a mechanism by which substrate binding can affect closure between the domains. Importantly, H273-E281 helix extends to the dimer interface as do several critical regions of the A and C domains. At the interface, these regions interact with their counterparts in the other subunit. Perhaps most interesting of all is the fact that the two active sites of the dimer appear to be in line with each other when viewed along the H273-E281 helix (Figure 5B). Thus, it is tempting to speculate that alteration of H273 disrupts the optimal interaction of the A and C domains, which through the dimer interface, effects the AIR binding site of the other subunit. Binding of AIR to one subunit should stabilize these interactions, which in turn, would help organize the AIR binding site of the other subunit, thus leading to positive cooperativity.

What is the Role of K353?

To date, we have mutated K353 to both alanine and arginine and in both cases, the mutant proteins are inactive. Proteolysis studies of the K353R protein indicated that the protein as folded, but likely displayed altered flexibility due to the change in the relative abundance of the protease cleavage fragments (Supplemental Information). While this could indicate that the K353 mutant did not adopt a conformation which allowed for substrate binding, K353A still bound AIR (7). A structural overlay of N^5-CAIR synthetase with biotin carboxylase indicates that K353 and R338 in biotin carboxylase occupy similar regions of the active site (side chain nitrogens are 2.5 Å apart). R338 has been extensively studied by site-directed mutagenesis (24, 29). Research has speculated that this residue is involved in carboxyphosphate stabilization. However, these studies have revealed that unlike the case with K353 in N^5-CAIR synthetase, mutant proteins of R338 still display activity and do not greatly alter the K_m for bicarbonate binding. Thus, K353 plays a more critical role in the mechanism of N^5-CAIR synthetase that the corresponding R338 plays in biotin carboxylase. We are currently conducting multilevel computational studies on the mechanism of N^5-CAIR synthetase that will hopefully shed light on the role of K353 in the mechanism of the enzyme.

Cooperativity and Regulation in N^5-CAIR Synthetase

Cooperativity in the ATP-grasp carboxylase enzymes has been the subject of much study (29). The kinetic results presented here are the first to indicate cooperativity between the two active sites in the functional dimer of N^5-CAIR synthetase. Unfortunately, cooperativity has not been detected for the wild-type enzyme. Cooperative interactions in biotin carboxylase have been investigated by making heterodimers in which one of the monomers is catalytically compromised (30). Studies by Janyani *et al.*, have shown that these heterodimers display only 5-25% activity which is significantly below the 50% activity that would be expected if the two subunits were independent (30). This supports the concept of intersubunit communication. Research by Shen *et al.*, however, showed that mutations which disrupt dimerization only resulted in a modest decrease in activity indicating that dimerization was not necessary for catalysis (31). A recent paper found that in an intracellular context, dimerization was required for growth in a biotin carboxylase deficient strain (20). This result indicated that dimerization was required for the ability of biotin carboxylase to interact with other proteins in the cell.

Biotin carboxylase has been shown to display negative cooperativity with respect to bicarbonate while N^5-CAIR synthetase displays positive cooperativity with regard to AIR binding. Positive cooperativity in N^5-CAIR synthetase would provide an advantage for this enzyme since it confers greater sensitivity to the concentration of AIR. Thus, changes in the concentration of AIR upon upregulation of the pathway would result in a larger enhancement in N^5-CAIR production.

The regulation of N^5-CAIR synthetase is an interesting issue. The product, N^5-CAIR, is unstable under physiological conditions and readily decarboxylates to regenerate AIR. This instability has lead to the suggestion that it may be channeled to the next enzyme in the pathway, N^5-CAIR mutase. However, channeling has not been detected for these enzymes, and research has shown that under conditions where the ratio of N^5-CAIR synthetase and N^5-CAIR mutase is 1:1, non-stoichiometric consumption of ATP occurs (11). Coupled with this observation is the fact that previous research has shown that N^5-CAIR can be synthesized non-enzymatically from AIR in the presence of elevated levels of CO_2(32). Indeed, N^5-CAIR synthetase mutants can be complemented by CO_2 indicating that N^5-CAIR synthetase is dispensable under certain conditions. The observation that N^5-CAIR synthetase is inhibited by high ATP concentrations and is cooperative with respect to AIR, may provide a mechanism to prevent the non-stoichiometric consumption of ATP by reducing the rate of N^5-CAIR synthesis to match the rate of N^5-CAIR consumption by N^5-CAIR mutase. When ATP levels are low, purine biosynthesis is upregulated, leading to an increase in AIR, which in turn would result in an increase in N^5-CAIR. The carbamate would ultimately be converted into IMP and then AMP, thus leading to an increase in ATP. Whether there are other regulatory systems controlling the synthesis of N^5-CAIR is the subject of future studies.

Supplementary Material

Refer to Web version on PubMed Central for supplementary material.

Acknowledgments

The authors thank Dr. Grover Waldrop and Dr. Hazel Holden for a critical reading of this manuscript.

References

1. Fawaz MV, Topper ME, Firestine SM. The ATP-grasp enzymes. Bioorg Chem. 2011; 39:185–191. [PubMed: 21920581]
2. Galperin MY, Koonin EV. A diverse superfamily of enzymes with ATP-dependent carboxylate-amine/thiol ligase activity. Protein Sci. 1997; 6:2639–2643. [PubMed: 9416615]
3. Murzin AG. Structural classification of proteins: New superfamilies. Curr Opin Struc Biol. 1996; 6:386–394.
4. Kappock TJ, Ealick SE, Stubbe J. Modular evolution of the purine biosynthetic pathway. Curr Opin Chem Biol. 2000; 4:567–572. [PubMed: 11006546]
5. Li H, Fast W, Benkovic SJ. Structural and functional modularity of proteins in the de novo purine biosynthetic pathway. Protein Sci. 2009; 18:881–892. [PubMed: 19384989]
6. Thoden JB, Holden HM, Firestine SM. Structural analysis of the active site geometry of N5-carboxyaminoimidazole ribonucleotide synthetase from Escherichia coli. Biochemistry. 2008; 47:13346–13353. [PubMed: 19053251]
7. Thoden JB, Holden HM, Paritala H, Firestine SM. Structural and Functional Studies of Aspergillus clavatus N-5-Carboxyaminoimidazole Ribonucleotide Synthetase. Biochemistry. 2010; 49:752–760. [PubMed: 20050602]
8. Firestine SM, Davisson VJ. Carboxylases in de novo purine biosynthesis Characterization of the Gallus gallus bifunctional enzyme. Biochemistry. 1994; 33:11917–11926. [PubMed: 7918410]

9. Bradford MM. A rapid and sensitive method for the quantitation of microgram quantities of protein utilizing the principle of protein-dye binding. Anal Biochem. 1976; 72:248–254. [PubMed: 942051]
10. Mueller EJ, Meyer E, Rudolph J, Davisson VJ, Stubbe J. N-5-Carboxyaminoimidazole Ribonucleotide: Evidence for a New Intermediate and two New Enzymatic Activities in the De Novo Purine Biosynthetic Pathway of Escherichia Coli. Biochemistry. 1994; 33:2269–2278. [PubMed: 8117684]
11. Firestine SM, Misialek S, Toffaletti DL, Klem TJ, Perfect JR, Davisson VJ. Biochemical role of the Cryptococcus neoformans ADE2 protein in fungal de novo purine biosynthesis. Arch Biochem Biophys. 1998; 351:123–134. [PubMed: 9500840]
12. Firestine SM, Paritala H, Mcdonnell JE, Thoden JB, Holden HM. Identification of inhibitors of N-5-carboxyaminoimidazole ribonucleotide synthetase by high-throughput screening. Bioorg Med Chem. 2009; 17:3317–3323. [PubMed: 19362848]
13. Attwood PV, Wallace JC. Chemical and catalytic mechanisms of carboxyl transfer reactions in biotin-dependent enzymes. Accounts Chem Res. 2002; 35:113–120.
14. Knowles JR. The Mechanism of Biotin-Dependent Enzymes. Annu Rev Biochem. 1989; 58:195–221. [PubMed: 2673009]
15. Raushel FM, Anderson PM, Villafranca JJ. Kinetic Mechanism of Escherichia-Coli Carbamoyl-Phosphate Synthetase. Biochemistry. 1978; 17:5587–5591. [PubMed: 215204]
16. Raushel FM, Mullins LS, Gibson GE. A stringent test for the nucleotide switch mechanism of carbamoyl phosphate synthetase. Biochemistry. 1998; 37:10272–10278. [PubMed: 9665735]
17. Climent I, Rubio V. ATPase activity of biotin carboxylase provides evidence for initial activation of bicarbonate by ATP in the carboxylation of biotin. Arch Biochem Biophys. 1986; 251:465–470. [PubMed: 2948446]
18. Gibson GE, Mullins LS, Raushel FM. Carbamoyl phosphate synthetase from Escherichia coli does not catalyze the dehydration of bicarbonate to carbon dioxide. Bioorg Chem. 1998; 26:255–268.
19. Blanchard CZ, Lee YM, Frantom PA, Waldrop GL. Mutations at four active site residues of biotin carboxylase abolish substrate-induced synergism by biotin. Biochemistry. 1999; 38:3393–3400. [PubMed: 10079084]
20. Smith AC, Cronan JE. Dimerization of the Bacterial Biotin Carboxylase Subunit Is Required for Acetyl Coenzyme A Carboxylase Activity In Vivo. J Bacteriol. 2012; 194:72–78. [PubMed: 22037404]
21. Janiyani K, Bordelon T, Waldrop GL, Cronan JE Jr. Function of Escherichia coli biotin carboxylase requires catalytic activity of both subunits of the homodimer. J Biol Chem. 2001; 276:29864–29870. [PubMed: 11390406]
22. LiCata VJ, Allewell NM. Is substrate inhibition a consequence of allostery in aspartate transcarbamylase? Biophys Chem. 1997; 64:225–234. [PubMed: 9127947]
23. Chou CY, Tong L. Structural and Biochemical Studies on the Regulation of Biotin Carboxylase by Substrate Inhibition and Dimerization. J Biol Chem. 2011; 286:24417–24425. [PubMed: 21592965]
24. Chou CY, Yu LPC, Tong L. Crystal Structure of Biotin Carboxylase in Complex with Substrates and Implications for Its Catalytic Mechanism. J Biol Chem. 2009; 284:11690–11697. [PubMed: 19213731]
25. Stapleton MA, JavidMajd F, Harmon MF, Hanks BA, Grahmann JL, Mullins LS, Raushel FM. Role of conserved residues within the carboxy phosphate domain of carbamoyl phosphate synthetase. Biochemistry. 1996; 35:14352–14361. [PubMed: 8916922]
26. Pastra-Landis SC, Evans DR, Lipscomb WN. The effect of pH on the cooperative behavior of aspartate transcarbamylase from Escherichia coli. J Biol Chem. 1978; 253:4624–4630. [PubMed: 26686]
27. Willemoes M. Thr-431 and Arg-433 are part of a conserved sequence motif of the glutamine amidotransferase domain of CTP synthases and are involved in GTP activation of the Lactococcus lactis enzyme. J Biol Chem. 2003; 278:9407–9411. [PubMed: 12522217]
28. Yifrach O, Horovitz A. Nested Cooperativity in the Atpase Activity of the Oligomeric Chaperonin Groel. Biochemistry. 1995; 34:5303–5308. [PubMed: 7727391]

29. Sloane V, Waldrop GL. Kinetic characterization of mutations found in propionic acidemia and methylcrotonylglycinuria - Evidence for cooperativity in biotin carboxylase. J Biol Chem. 2004; 279:15772–15778. [PubMed: 14960587]

30. Janiyani K, Bordelon T, Waldrop GL, Cronan JE. Function of Escherichia coli biotin carboxylase requires catalytic activity of both subunits of the homodimer. J Biol Chem. 2001; 276:29864–29870. [PubMed: 11390406]

31. Shen Y, Chou CY, Chang GG, Tong L. Is dimerization required for the catalytic activity of bacterial biotin carboxylase? Mol Cell. 2006; 22:807–818. [PubMed: 16793549]

32. Firestine SM, Poon SW, Mueller EJ, Stubbe J, Davisson VJ. Reactions Catalyzed by 5-Aminoimidazole Ribonucleotide Carboxylases from Escherichia Coli and GallusGallus: a Case for Divergent Catalytic Mechanisms. Biochemistry. 1994; 33:11927–11934. [PubMed: 7918411]

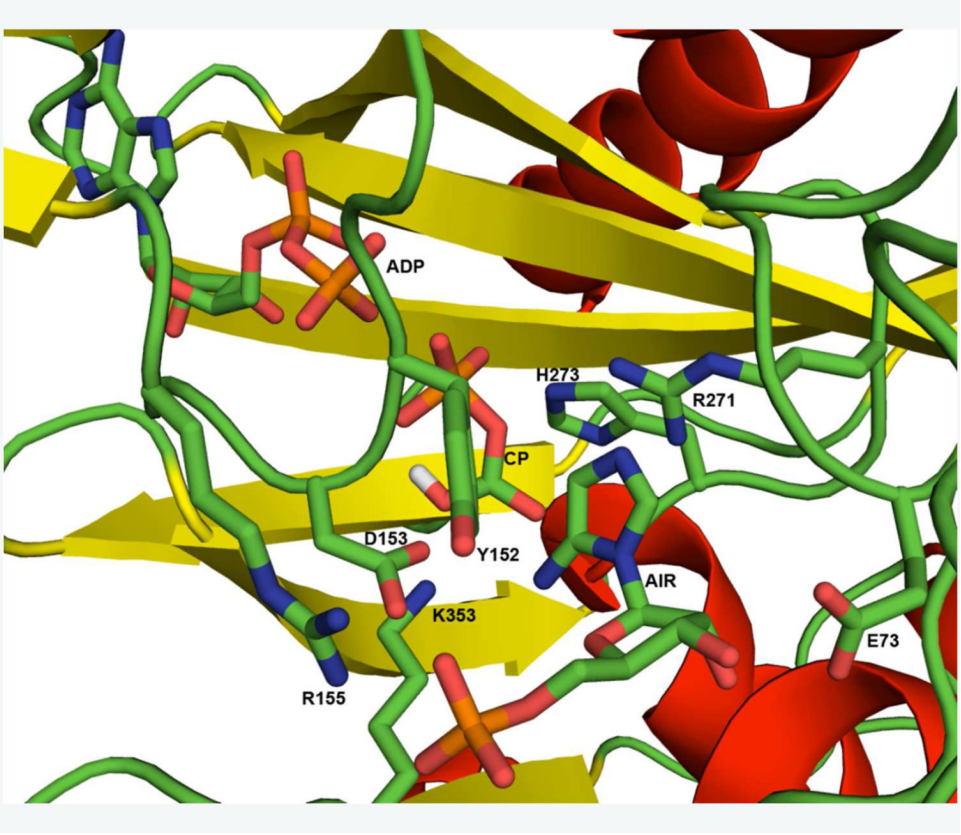

Figure 1. The active site of N^5-CAIR synthetase modeled with carboxyphosphate (CP)

The crystal structure of *Aspergillus* N^5-CAIR synthetase with bound ADP and AIR (3K5I) was superimposed with the crystal structure of *E. coli* N^5-CAIR synthetase with bound ADP and Pi (3ETJ). The location of inorganic phosphate, which was generated by the ATPase activity of N^5-CAIR synthetase in the crystal, was taken as the location of the phosphate group of carboxyphosphate. A minimized structure of carboxyphosphate was then superimposed onto the phosphate group to generate the model shown. All groups, with the exception of caroxyphosphate (CP) are shown as they exist in 3K5I. Residues that were mutated are shown as sticks and are labeled.

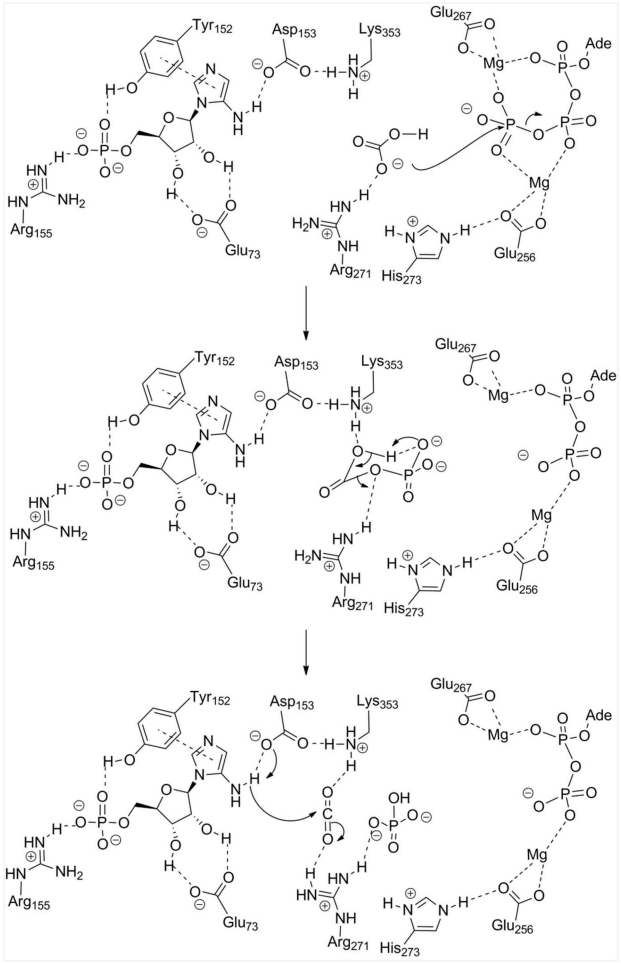

Figure 2.
Proposed mechanism of N^5-CAIR synthetase based upon the available crystal structures and the model shown in Figure 1.

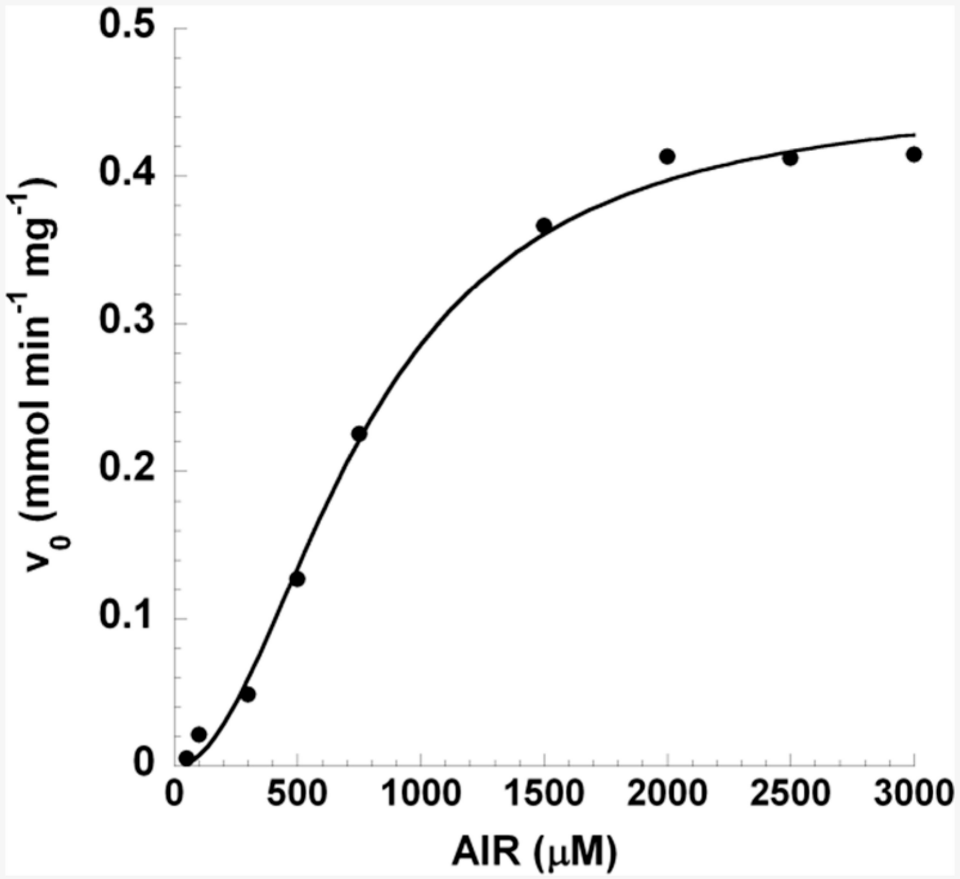

Figure 3. Initial velocity of the full reaction catalyzed by N^5-CAIR synthetase H273A mutant protein at constant ATP and bicarbonate but various AIR concentrations

The data were fitted to equation 2.

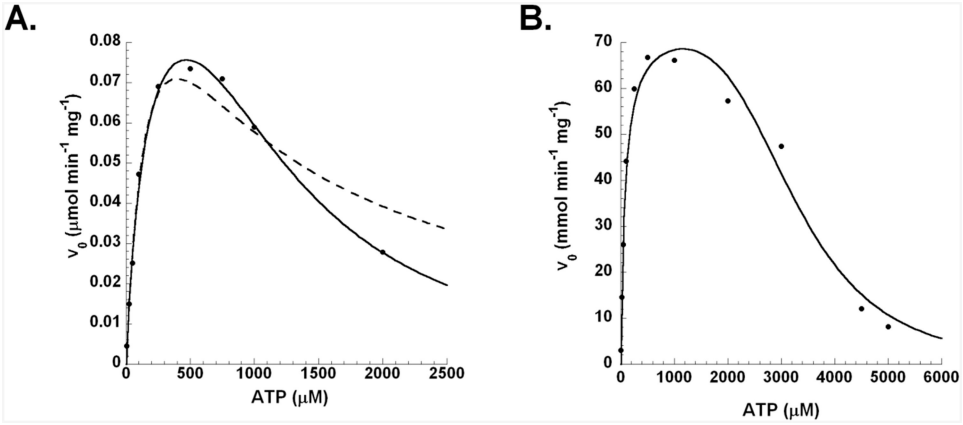

Figure 4. Initial velocity of the full reaction (as a function of ATP) catalyzed by N^5-CAIR synthetase R271K mutant enzyme (A) wild-type enzyme (B) at constant AIR and bicarbonate concentrations

For **A**, the data were fit to either the equation for substrate inhibition (eq 3, dashed line) and/or the equation for substrate inhibition where the inhibiting substrate is cooperative (eq. 5, solid line, n=2). For the wild-type enzyme, the data were fit to eq. 5 with n=4.

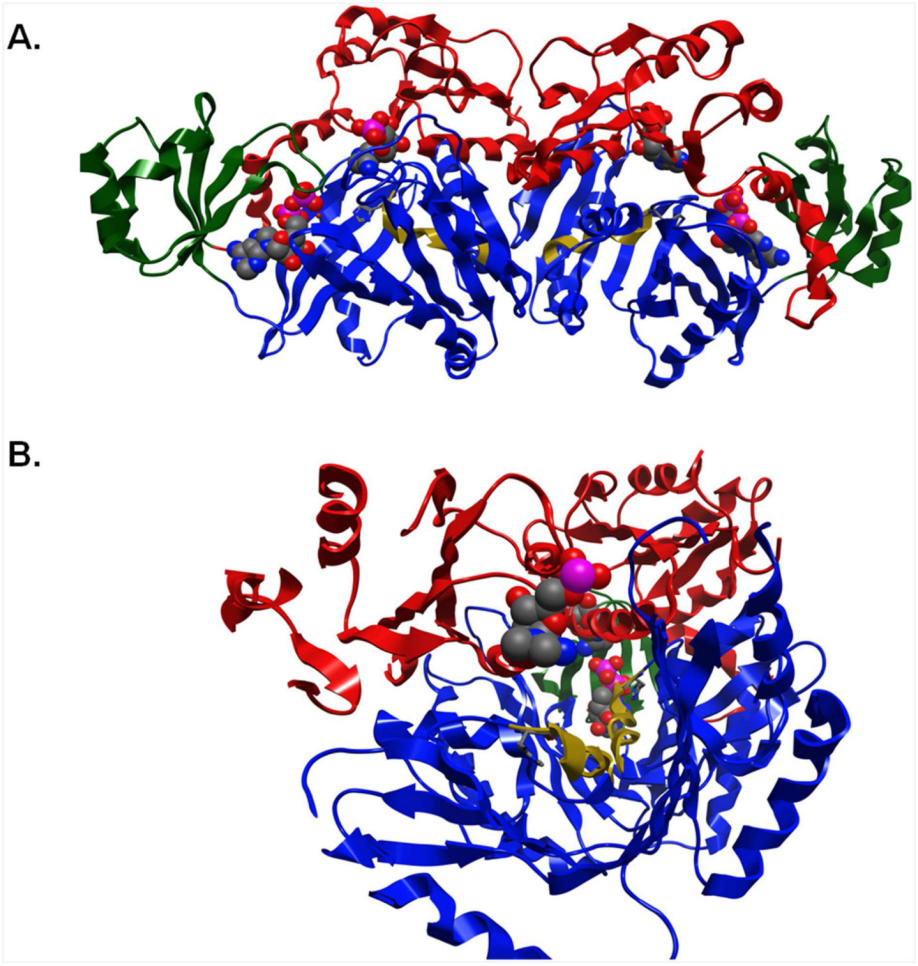

Figure 5. Structure of N^5-CAIR synthetase dimer

A. The A, B, and C domains of each subunit are shown in red, green and blue respectively. AIR and ATP are shown in spacefilling representation, while H273 is shown in the stick representation. The H273-E-281 helix is shown in gold. B. The view down the H273-E281 helix. Notice that the two helices (gold) are pointing at the other active site. The AIR of one subunit is shown in the front, while the second is shown in the center behind the second helix. This picture was created by rotating to the B-domain and Z-clipping the domain to gain access to the AIR binding site.

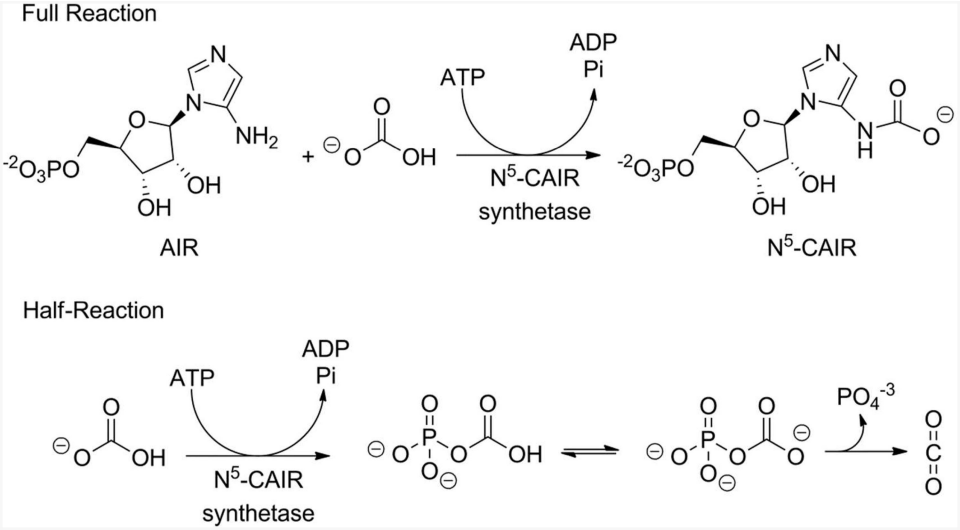

Scheme 1. Full and half-reactions of N^5-CAIR synthetase

Table 1

Kinetic parameters for wild-type enzyme and mutant proteins for half reaction with HCO_3^- varied[a]

	V_{max}[b] (μmol min^{-1}mg^{-1})	K_m[b](mM)	K_m (fold change)	K_{cat}[c] (min^{-1})	K_{cat}/K_m (μM^{-1} min^{-1})	K_{cat}/K_m (fold change)
wild-type	0.043 ± 0.002	3.9 ± 0.5	0	3.8 ± 0.2	1 ± 0.4	1
E73A	0.17 ± 0.01	33 ± 6	9	15 ± 1	0.5 ± 0.2	2
Y152A	0.03 ± 0.0007	5 ± 0.3	1	1.9 ± 0.04	0.4 ± 0.1	3
Y152F	0.05 ± 0.001	2.8 ± 0.02	1	3.2 ± 0.08	1 ± 0.4	1
D153A	0.15 ± 0.01	15 ± 4	4	14 ± 1	0.9 ± 0.3	1
R155A	0.10 ± .003	7 ± 0.7	2	8.6 ± 0.3	1 ± 0.4	1
R271A	Inactive[d]	nd	nd	nd	nd	nd
R271Q	Inactive[d]	nd	nd	nd	nd	nd
R271K	0.0009 ± 0.00008	80 ± 20	22	0.08 ± 0.007	0.001 ± 0.0004	1,000
H273A	Inactive[d]	nd	nd	nd	nd	nd
H273Q	Inactive[d]	nd	nd	nd	nd	nd
K353A	Inactive[d]	nd	nd	nd	nd	nd
K353R	Inactive[d]	nd	nd	nd	nd	nd

[a] Reported data are average of duplicates and errors are those obtained from curve fitting (equation 1) the appropriate data set.

[b] Steadystate values were determined using the ATP coupled assay system without AIR, with the concentration of ATP fixed and the concentration of bicarbonate is varied. K_m values are derived from the total amount of bicarbonate in solution (including background and added bicarbonate).

[c] Calculated using the molecular weight of the dimer.

[d] No measurable activity up to a protein concentration of 700- 4500 μg/mL.

Table 2

Kinetic parameters for wild-type enzyme and mutant proteins for the full reaction with AIR varied[a]

	V_{max}[b] (μmol min^{-1}mg^{-1})	K_m[b] (μM)	K_m (fold change)	K_{cat}[c] (min^{-1})	K_{cat}/K_m (μM^{-1} min^{-1})	K_{cat}/K_m (fold change)
wild-type	55 ± 3	22 ± 4	0	5,000 ± 270	230 ± 68	1
Y152A[e]	1 ± 0.2	460 ± 120	18	110 ± 20	0.50 ± 0.2	460
Y152F	18 ± 0.5	68 ± 6	3	1,600 ± 45	24 ± 8	8.5
R271A	0.0013 ± 0.00008	254 ± 53	12	0.11 ± 0.007	0.0005 ± 0.0001	460,000
R271Q	0.004 ± 0.0003	87 ± 19	4	0.4 ± 0.03	0.004 ± 0.001	57,500
R271K	0.33 ± 0.02	608 ± 83	28	50 ± 2	0.076 ± 0.03	3,030
H273A[e]	0.41 ± 0.01	742 ± 51	34	26 ± 0.9	0.036 ± 0.02	6,400
H273Q	0.0022 ± 0.00008	28 ± 4	1	0.19 ± 0.007	0.007 ± 0.002	32,900
K353A[f]	Inactive	nd	nd	nd	nd	nd
K353R	Inactive[d]	nd	nd	nd	nd	nd

[a] Reported data are average of duplicates and errors are those obtained from curve fitting (equation 1) the appropriate data set.

[b] Steady-state values were determined using the ATP coupled assay system with the concentration of ATP and bicarbonate fixed and the concentration of AIR is varied.

[c] Calculated using the molecular weight of the dimer.

[d] No measurable activity up to a protein concentration of 700 μg/mL.

[e] Kinetic parameters obtained using equation 2.

[f] Ref. No (7)

Table 3

Kinetic parameters for wild-type enzyme and mutant proteins for the full reaction with ATP varied[a]

	V_{max}[b] (μmol min^{-1}mg^{-1})	K_m[b] (μM)	K_m (fold change)	K_{cat}[c] (min^{-1})	K_{cat}/K_m (μM^{-1} min^{-1})	K_{cat}/K_m (fold change)
wild-type	79 ± 3	59 ± 8	0	7,100 ± 230	120 ± 31	1
R271A	0.0011 ± 0.0001	213 ± 37	4	0.099 ± 0.005	0.0005 ± 0.0001	240,000
R271Q	0.0014 ± 0.0001	108 ± 28	2	0.13 ± 0.009	0.001 ± 0.0003	120,000
R271K[d]	0.11 ± 0.006	131 ± 16	2	9.5 ± 0.5	0.074 ± 0.03	1,600
H273A	0.26 ± 0.02	175 ± 39	3	23 ± 2	0.13 ± 0.04	920
H273Q	0.003 ± 0.0001	95 ± 17	2	0.2 ± 0.008	0.002 ± 0.0005	60,000

[a] Reported data are average of duplicates and errors are those obtained from curve fitting (equation 1) the appropriate data set.

[b] Steady-state values were determined using the ATP coupled assay system with the concentration of AIR (fixed at K_m) and bicarbonate fixed and the concentration of ATP is varied.

[c] Calculated using the molecular weight of the dimer.

[d] Kinetic parameters obtained using equation 3